NON-CONTACT HARMONIC DETECTION OF FERROMAGNETIC MATERIAL DEFECTS BASED ON SQGSR AND OPLTF

Yizhen Zhao, Xinhua Wang, Yingchun Chen, Haiyang Ju, Yi Shuai

Beijing University of Technology, College of Mechanical Engineering and Applied Electronics Technology,
100 Ping Le Yuan, Chaoyang District, Beijing 100124, China (zyzbjut926@163.com, ✉ paper_bgdjd103@163.com,
+86 010 6793 6214, ychen08089@163.com, haiyoung.ju@gmail.com, shuaiyi_cjdx2008@126.com)

Abstract

In order to find the defects in ferromagnetic materials, a non-contact harmonic detection method is proposed. According to the principle of frequency modulated carrier wave, a tunnel magneto resistance harmonic focusing vector array detector was designed which radiates lower and higher frequency electromagnetic waves through the coil array to the detection targets. We use bistable stochastic resonance to enhance the energy of collected weak target signal and apply quantum computation and a Sobol low deviation sequence to improve genetic algorithm performance. Then we use the orthogonal phase-locked loop to eliminate the intrinsic background excitation field and tensor calculations to fuse the vector array signal. The finite element model of array detector and the magnetic dipole harmonic numerical model were also established. The simulation results show that the target signal can be identified effectively, its focusing performance is improved by 2 times, and the average signal-to-noise ratio is improved by 9.6 times after the algorithm processing. For the experiments, we take Q235 steel pipeline as the object to realize the recognition of three defects. Compared with the traditional methods, the proposed method is more effective for ferromagnetic materials defects detection.

Keywords: harmonic detection, ferromagnetic materials defects, focusing vector array, signal extraction algorithm.

1. Introduction

Ferromagnetic materials are widely used in engineering structures. However, they inevitably cause defects in the process of manufacturing and using which will seriously threaten ,safe operation of equipment. In order to avoid the occurrence of industrial accidents, it is necessary perform regular checks of ferromagnetic components. As a typical ferromagnetic material component, the steel oil and gas pipeline has a long laying distance and a long service life. Under the influence of internal and external corrosion, human damage and other factors, it will develop defects in the pipeline body, such as sunken deformations, cracks, perforations and so on. Conventional *Non-*

Destructive Testing (NDT) methods include x-ray testing [1], ultrasonic testing [2, 3], magnetic particle testing [4], penetrant testing [5] and eddy current testing [6, 7]. These traditional detection methods have some limitations in practical engineering applications such as radiation harmful to the human body, surface contamination of components with the coupling agent, skin effect of eddy current and so on. With the development of science and technology, pipeline internal inspection technology [8, 9] has been applied to some important pipelines using devices called smart pigs. However, due to the limitations of space and turning angle, a smart pig is prone to congestion or loss and its cost is extremely high. In the pipeline external detection technology, *Transient Electromagnetic Method* (TEM) can detect defects such as wall thickness thinning and pipeline body cracks [10]. However, due to the attenuation and discontinuity of its signal characteristics, it still needs further research and improvement. *Magnetic Tomography Method* (MTM) and *Geomagnetic Method* (GM) are passive detection technologies based on environmental magnetic field [11, 12] which are easy to operate and can reflect stress concentration areas. But the passive magnetic field is very weak and the method's resistance to interference is poor which makes the detection signal vulnerable to external interference and effective information difficult to extract.

In addition, shaking of the detector and the noise in the environment reduces the the degree of effective identification of pipeline defects targets in actual engineering detection. Therefore, it is necessary to adopt an appropriate signal processing algorithm to extract defects. Song [13] introduced *Wavelet Transform* (WT) to process the magnetic field signal component and identified crack defects in a high-pressure pipeline. Huang [14] used *Empirical Mode Decomposition* (EMD) to identify porosity defects in aluminium alloy welds. Amirat [15] used *Ensemble Empirical Mode Decomposition* (EEMD) to eliminate the inherent modal order limit to perform effective signal decomposition and this approach was successfully applied in bearing fault detection. Different from the traditional filtering method, *Stochastic Resonance* (SR) can transfer the noise energy to the target signal, improve the *Signal-to-Noise Ratio* (SNR) of the original signal, so as to achieve extraction of weak signal [16–18]. Wan [19] used the bistable SR to extract the weak magnetic anomaly signal. Shi [20] used EMD and SR to eliminate noise and extract characteristic signals which was successfully applied to fault diagnosis. Li [21] introduced *Genetic Algorithm* (GA) into the SR system to optimize parameters automatically which was used for on-line detection of blade crack defects. Yin [22, 23] established a cross-shaped vector sensor array for *Tensor Fusion* (TF) and correction to achieve high-precision target positioning.

This paper presents a non-contact harmonic detection method for defects of ferromagnetic materials. A harmonic- focused vector array detector was designed which radiates lower frequency (several tens of Hz) and higher frequency (several kHz) electromagnetic waves through a coil array to the targets according to the principle of *Frequency Modulated Carrier Wave* (FMCW), and a high-sensitivity *Tunnel Magneto Resistance* (TMR) vector sensor array was used for parallel signal acquisition. Then, the bistable SR was used to enhance the energy of the weak target signal. The GA was used to optimize the parameters adaptively, and improved by quantum computation and Sobol low deviation sequence. Finally, *Orthogonal Phase-Locked* (OPL) was used to eliminate the background excitation field and the vector array signals were processed with TF, so as to identifiy of ferromagnetic material defect targets.

2. Principle of harmonic detection

The non-contact harmonic detection of ferromagnetic materials defects is an electromagnetic NDT method based on the principle of FMCW [24]. Harmonic excitation signal combines the characteristics of lower and higher frequency electromagnetic wave which can improve the

detection sensitivity and resolution and overcome the skin effect limitation. It can realize the detection of defects on the surface or subsurface of ferromagnetic materials. The harmonic excitation signal $f(t)$ is generated by superposition of multiple sine signals and its mathematical analytical model can be expressed as:

$$f(t) = \sum_{i=0}^{n} f_i(t) = \sum_{i=0}^{n} A_i \sin(2\pi f_i t + \theta_i), \tag{1}$$

where i is the number of sine wave synthesis, A_i is the amplitude, f_i is the frequency, and θ_i is the initial phase angle. The harmonic focused vector array detector is used to radiate the excitation signal with higher energy density to the object to be detected and obtain the reflected echo signal. The detector structure is shown in Fig. 1a and the focusing effect is shown in Fig. 1b.
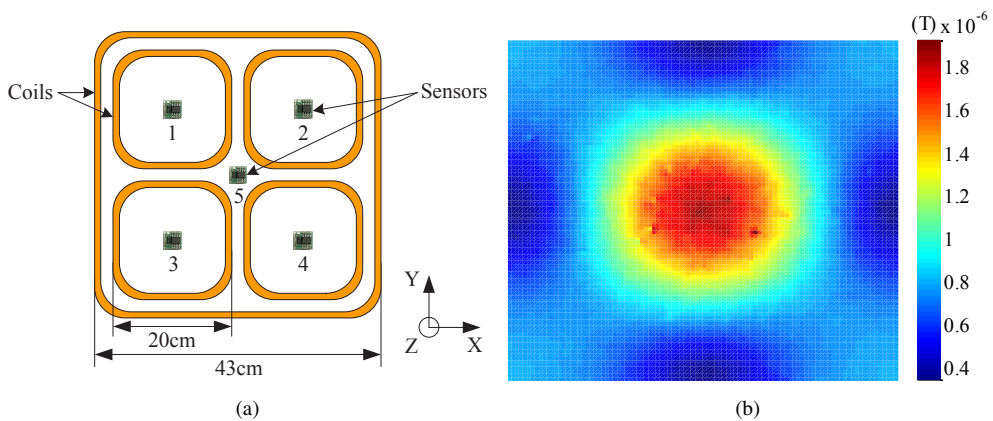

Fig. 1. The harmonic focused vector array detector: (a) actual structure; (b) focusing effect under the condition of a 2 A current and lifting height 100 cm.

A three-dimensional (3D) Cartesian coordinate system is established with the center of the array as the origin. The finite element simulation of the array and the non-array excitation probe are compared under different lift-off heights. Within the range of [–50, 50] cm detection line below the detector, the lifting height is set at 30 cm, 50 cm and 70 cm respectively. The focusing enhancement effect is shown in Fig. 2. It can be seen that the harmonic flux density module decreases gradually, the performance of the excitation focusing array is about two times better than that of the non-array probe and the effective excitation coverage area is bigger under the same excitation intensity. Therefore, the principle of array focusing detection is feasible.

As steel is a typical ferromagnetic material, the defects in a steel pipeline disturb the original wave field and reflect it in the receiving sensors under the excitation of different harmonic components which can cause exceptions to the local signal. However, pipeline detection work is complicated and changeable. Target signal exists mostly in the form of nonlinear, non-stationary and low SNR which makes effective extraction of abnormal signals very difficult. According to its vector characteristics, the pipeline radial, axial and circumferential 3D signals are collected. Then an appropriate algorithm is used to extract the abnormal signal and identify the location of the pipeline defects target source. The detection principle is shown in Fig. 3.
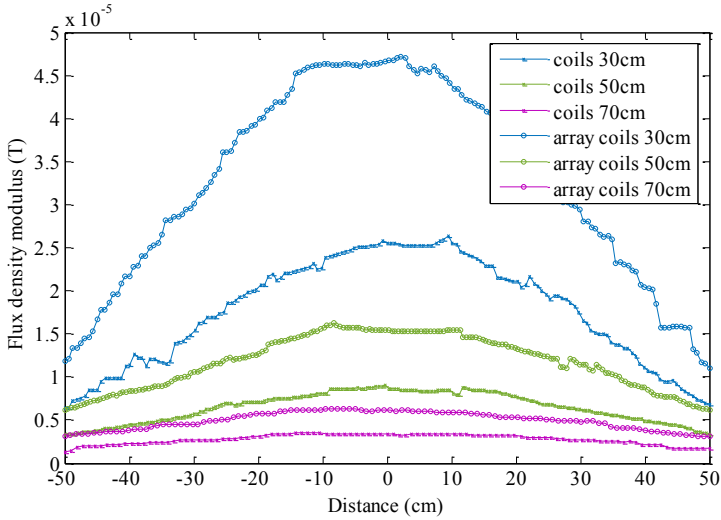
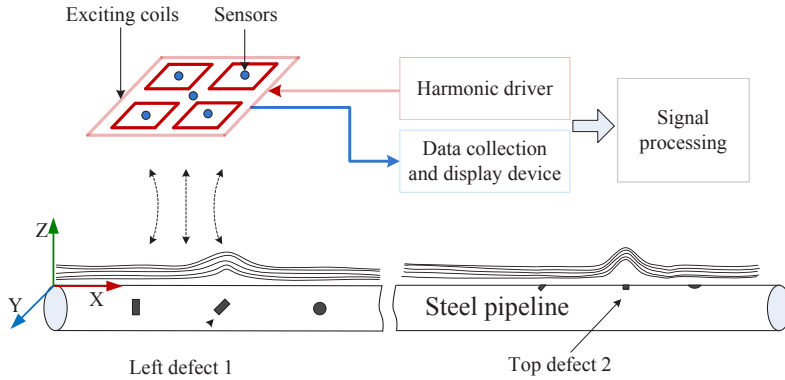Fig. 2. The focusing enhancement effect of array.

Fig. 3. The principle of harmonic detection.

3. Defect target signal extraction algorithm

3.1. Bistable variable scale time domain stochastic resonance

Different from the traditional filtering and denoising methods, the SR is based on energy transfer mechanism which can transfer noise energy to the target signal and generate a stochastic resonance spectrum peak. It is suitable for weak target signal enhancement and extraction under strong background noise. Considering the changes in the periodic signal and noise, the classical nonlinear bistable system can be expressed as follows [25]:

$$\begin{cases} \dfrac{\mathrm{d}x}{\mathrm{d}t} = -\dfrac{\mathrm{d}U(x)}{\mathrm{d}t} + s(t) + n(t) \\ U(x) = -\dfrac{a}{2}x^2 + \dfrac{b}{4}x^4 \end{cases}, \tag{2}$$

where $x(t)$ is the output signal of system, $s(t)$ is the periodic signal, $n(t)$ is the noise, $U(x)$ is the potential function; a and b are non-negative system parameters. By adjusting the parameters of the system, the barrier height and the width of the potential well can be changed, as shown in Fig. 4. The larger the parameter a or the smaller the parameter b, the wider the potential well and the higher the potential barrier. When the value of parameter a continues to decrease, the transition from bistable to monostable can be realized.
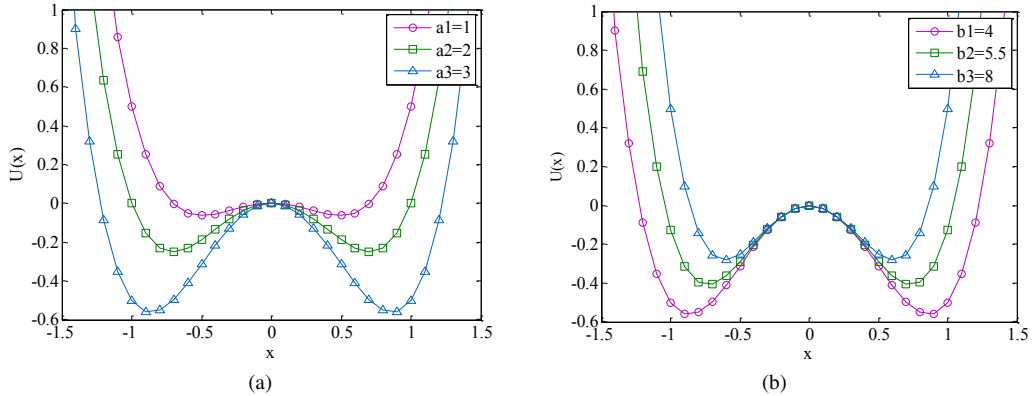

(a)　　　　　　　　　　　　　　　　　　　　(b)

Fig. 4. The change of potential function under different parameter settings: a) $b = 4$, $a_1 = 1$, $a_2 = 2$, $a_3 = 3$;
b) $a = 3$, $b_1 = 4$, $b_2 = 5.5$, $b_3 = 8$.

The actual collected signals are all mixed with noise, so let $sn(t) = s(t) + n(t)$ in the SR system. Then it is solved with the high-precision fourth-order Runge–Kutta method which is described as follows:

$$
\begin{cases}
x_{n+1} = x_n + \dfrac{h}{6}(K_1 + 2K_2 + 2K_3 + K_4) \\[2mm]
K_1 = ax_n - bx_n^3 + sn_n \\[2mm]
K_2 = a\left(x_n + \dfrac{K_1}{2}\right) - b\left(x_n + \dfrac{K_1}{2}\right)^3 + sn_n \\[2mm]
K_3 = a\left(x_n + \dfrac{K_2}{2}\right) - b\left(x_n + \dfrac{K_2}{2}\right)^3 + sn_{n+1} \\[2mm]
K_4 = a\left(x_n + K_3\right) - b(x_n + K_3)^3 + sn_{n+1}
\end{cases}, \tag{3}
$$

where h is the iteration step size, x_n is the output signal of the SR system.

The acquisition of harmonic signal must meet the Nyquist sampling theorem, so it cannot be the directly input signal of the SR system [26]. Therefore, a linear compression method based on variable scale was proposed. Assuming that the signal frequency $f_0 > 1$, the sampling frequency f_s, an appropriate scaling coefficient K needs to be selected for linear compression. Then the secondary sampling frequency is changed to $f_{sk} = f_s/K$. So the signal frequency domain becomes $f_0' = f_0/K < 1$. The scale-varying process of a signal can be expressed as follows:

$$
s(t) = A\sin(\omega t) = A\sin\left(2\pi f_0 \frac{n}{f_s}\right) = A\sin\left[2\pi\left(\frac{f_0}{K}\right)\left(n/\frac{f_s}{K}\right)\right], \tag{4}
$$

where n is the number of sampling points, $n = 0, 1, 2, \ldots, N - 1$. When scaling, the calculation step size of the Runge–Kutta is adjusted, which has no effect on the signal property.

After scaling, the output signal of the SR system will be distorted in the time domain, while the actual harmonic detection method is more sensitive to the time domain signal. It is necessary to introduce a time domain recovery system to restore the signal in order to more intuitively represent the defect information. When the noise $n(t)$ is close to 0, the time-domain waveform can be obtained by calculating the response of a recovery system to the distorted signal. The recovery system function $r(x)$ was introduced, and its time track coincides with the input signal $s(t)$, which can be defined as follows:

$$r(x) = -ax + bx^3 = U'(x). \tag{5}$$

The recovery system function $r(x)$ is formally expressed as the first derivative of the bistable system potential function $U(x)$.

3.2. Adaptive parameters optimization

In order to achieve an ideal output state of the system, an adaptive optimization algorithm was used to select the parameters a, b and scale h of the bistable SR system instead of an arbitrary one. Based on quantum computation and genetic algorithm, the Quantum Genetic Algorithm (QGA) introduces the quantum vector state into genetic coding and uses the rotation strategy of the quantum gate to realize population evolution and data updating [27]. The states of qubits can be expressed as follows:

$$\begin{cases} |\psi\rangle = \alpha |0\rangle + \beta |1\rangle \\ |\alpha|^2 + |\beta|^2 = 1 \end{cases}, \tag{6}$$

where ψ represents the quantum state, α and β represent the probability amplitude of the corresponding state. The initial state is $\alpha = \beta = 1/\sqrt{2}$.

A chromosome can be composed of multiple quantum codes, known as chromosome length. Population evolution is realized by a quantum rotation matrix and the rotation gate and transformation process are as follows:

$$\begin{bmatrix} \alpha_i' \\ \beta_i' \end{bmatrix} = U(\theta_i) \begin{bmatrix} \alpha_i \\ \beta_i \end{bmatrix} = \begin{bmatrix} \cos(\theta_i) & -\sin(\theta_i) \\ \sin(\theta_i) & \cos(\theta_i) \end{bmatrix} \begin{bmatrix} \alpha_i \\ \beta_i \end{bmatrix}, \tag{7}$$

where θ_i is the rotation angle, $\begin{bmatrix} \alpha_i & \beta_i \end{bmatrix}^T$ is the probability amplitude of gene i. The direction and value of θ are determined by the rotation strategy, [28] which is shown in Table 1.

In order to conform to the evolution characteristics of real population, *Sobol Quantum Genetic Algorithm* (SQGA) was used to improve the population randomness and uniformity of QGA by a Sobol low discrepancy sequence which provides better sample distribution [29]. This algorithm has not only a high-quality solution but a fast convergence of quantum optimization as well. Distribution of sample points of the Sobol sequence is shown in Fig. 5.

In the binary coding quantum state of SQGA, if $\alpha_i^2 \leq \varepsilon_i$, the binary encoding is set to 0 in the update strategy, otherwise it is set to 1, where ε_i is generated randomly in the Sobol sequence, and $0 < \varepsilon_i < 1$. The improved algorithm makes the evolution process follow certain rules and can suppress the random error. During the data update, the SNR is used as fitness evaluation function

Table 1. Quantum rotation gate strategy.

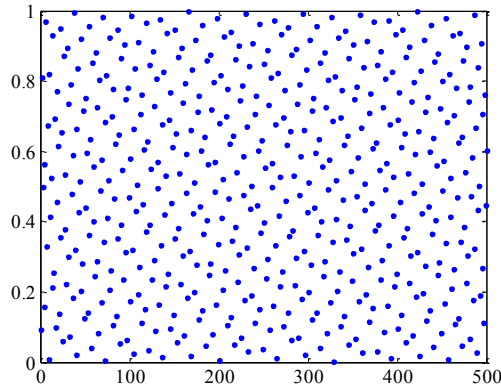| x_i	$best_i$	$f(x) \geq f(best)$	$\Delta\theta_i$	$s(\alpha_i, \beta_i)$				
				$\alpha_i\beta_i > 0$	$\alpha_i\beta_i < 0$	$\alpha_i = 0$	$\beta_i = 0$	
0	0	false	0	0	0	0	0	
0	0	true	0	0	0	0	0	
0	1	false	0.01π	+1	−1	0	±1	
0	1	true	0.01π	−1	+1	±1	0	
1	0	false	0.01π	−1	+1	±1	0	
1	0	true	0.01π	+1	−1	0	±1	
1	1	false	0	0	0	0	0	
1	1	true	0	0	0	0	0	

Fig. 5. The Sobol sequence distribution.

which is calculated as follows:

$$
\text{SNR} = 10\log\left\{ \frac{\sum_{n=1}^{N} s^2(n)}{\sum_{n=1}^{N} [s(n) - \hat{s}(n)]^2} \right\},
\tag{8}
$$

where $s(n)$ is the original input signal and $\hat{s}(n)$ is the signal processed by Sobol Quantum Genetic Stochastic Resonance (SQGSR).

3.3. Orthogonal phase-locked tensor fusion

Although harmonic detection brings benefits, it is inevitable to introduce an excitation signal field in the processing. According to the principle of electromagnetic detection, the frequency components are deterministic and controllable. The OPL method based on the correlation detection can effectively suppress the excitation background field, so as to extract the damage target signals, as shown in Fig. 6.
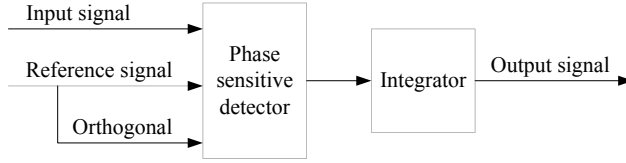
Fig. 6. The principle of OPL.

The cores of the OPL are a phase-sensitive detector and an integrator whose functions are performed by an analog multiplier and a low-pass filter respectively. Suppose the input harmonic detection signal $S(t)$ and the reference signal $R(t)$ are as below:

$$\begin{cases} S(t) = A\sin(\omega_0 t + \varphi) + B\sin(\omega_1 t + \varphi) + N(t) \\ R(t) = C\sin(\omega_2 t + \varphi + \theta) \end{cases}, \tag{9}$$

where A, B and C are amplitude, ω is angular frequency, θ is the phase difference between reference signal and harmonic signal. Under the condition that the actual phase angle of the detected signal is unknown, the orthogonal method is used to eliminate the influence of the phase difference. First, we multiply the input signal and the reference signal of the same frequency, then we apply the orthogonal phase-lock loop to the reference signal itself and multiply it with the input signal again, which is expressed as:

$$\begin{cases} V(t) = S(t) \cdot R(t) \\ V_\perp(t) = S(t) \cdot R_\perp(t) \end{cases}. \tag{10}$$

When $\omega_0 = \omega_2$, the demodulated signal contains *direct current* (DC) signal, differential frequency signal and double frequency signal. By using the low-pass filter and setting an appropriate cut-off frequency, the DC signal component can be obtained. Then, the phase of reference signal shift $\pi/2$, the dynamic analysis of the signal can be completed without considering the initial phase difference. Therefore,

$$AC = 2\sqrt{V^2 + V_\perp^2}. \tag{11}$$

Similarly, when $\omega_1 = \omega_2$, we get BC. Then the excitation background signals in harmonic detection can be eliminated.

In addition, the direction sensitivity of harmonic detection signals with different defects types in the pipeline is different. The vector array is used to eliminate the error caused by the direction of spatial signals and the TF algorithm is adopted to enhance the directivity of the target signal source [30]. As a vector field with continuous distribution in space, harmonic magnetic field can be expressed as:

$$B(x, y, z) = B_x(x, y, z)i + B_y(x, y, z)j + B_z(x, y, z)k, \tag{12}$$

where i, j and k represent the unit vectors in the x, y and z directions respectively.

Under the condition of instantaneous local signal sampling, the actual vector array can directly obtain the triaxial signal components of harmonic magnetic field. Using the idea of difference equivalence to calculate the gradients in different directions of triaxial signals, the tensor matrix G can be obtained as follows:

$$G = \begin{bmatrix} \partial B_x/\partial x & \partial B_x/\partial y & \partial B_x/\partial z \\ \partial B_y/\partial x & \partial B_y/\partial y & \partial B_y/\partial z \\ \partial B_z/\partial x & \partial B_z/\partial y & \partial B_z/\partial z \end{bmatrix} = \begin{bmatrix} B_{xx} & B_{xy} & B_{xz} \\ B_{yx} & B_{yy} & B_{yz} \\ B_{zx} & B_{zy} & B_{zz} \end{bmatrix}. \tag{13}$$

The modulus of the tensor is not affected by the background magnetic field and the detection angle deviation and its maximum value can be used as one of the criteria to determine the pipeline defects which can be expressed as:

$$S_{target} = \max \sqrt{\sum (B_{ij})^2} \quad i, j = x, y, z. \tag{14}$$

4. Simulation and analysis

Usually, the place of application of the non-contact harmonic detection method is relatively distant from the defect targets of the pipeline. Thus a far-field magnetic dipole and FMCW are used to construct a harmonic detection signal model described as:

$$S_0 = \frac{\mu_0}{4\pi} \left[\frac{3(\boldsymbol{M} \cdot \boldsymbol{r})\boldsymbol{r}}{r^5} - \frac{\boldsymbol{M}}{r^3} \right] + \sum_{i=1,2} A_i \sin(2\pi f_i t + \theta_i) + n(t). \tag{15}$$

where μ_0 is the permeability of vacuum; $\boldsymbol{M}$ is the magnetic moment; $\boldsymbol{r}$ is the vector diameter from the origin to the detection point; $r = |\boldsymbol{r}|$; A_i, f_i, and θ_i are the amplitude, frequency and initial phase of the harmonic components respectively and $n(t)$ is noise. The magnetic moment will change under the harmonic excitation, but this model only makes qualitative analysis on the extraction of defect target signal, so the result is not affected.

In the simulation model, the length of the pipeline is 5 m, the wall thickness is 1 cm, the diameter is 20 cm, and two defects source are designed on the pipeline. The horizontal detection length is 5 m, and the vertical lifting height is 1 m. In the magnetic dipole, the magnetic moment is set to $[277, -29, 726]$, the amplitude of the first harmonic component is 2, the frequency is 23 Hz, the initial phase is 0, the amplitude of the second harmonic component is 3, the frequency is 1 kHz, the initial phase is 0, and a noise with SNR = 2 dB is added. After normalization of the data collected by the center sensor of the 3D vector detection array, as shown in Fig. 7. One can see there that the defect targets are completely submerged and cannot be identified directly.
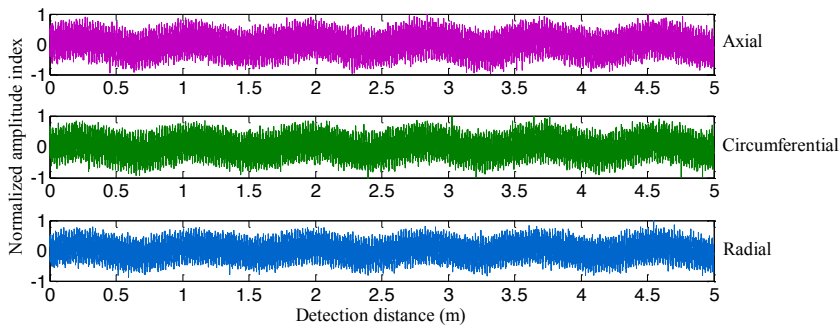

Fig. 7. Simulation data acquisition.

Next, we take the radial signal of array center sensor as an example and discuss in detail. First, a fourth-order Butterworth low-pass filter is used to select the frequency of the signal and the cut-off frequency f_s is set to 5 kHz. Then SQGSR is used to enhance the weak target signal. The optimization interval of each parameter is set as $a \in (0, 10]$, $b \in [10, 20]$, $h \cdot f_s \in [5\,000, 10\,000]$, the maximum genetic algebra is 30, the population size is 50, and the chromosome length is 20. The optimal solution of system output is shown in Table 2.

Table 2. Optimal solution of SQGSR.

	a	b	$h \cdot f_s$	SNR
Axial	5.16	16.95	7486.33	19.26
Circumferential	5.54	19.46	6957.78	19.22
Radial	4.29	13.55	8937.32	19.31

With the signal processed by SQGSR, the target signal can be enhanced effectively and the SNR is increased by 9.6 times on average. After recovery of the system in the time-domain, the radial signal of the array center sensor is shown in Fig. 8a. In the process of parameter optimization, SQGA plays a significant role in improving the performance of traditional a GA. It can rapidly converge to the optimal solution with smaller population size and shorter time, and the optimal SNR value is larger with the same genetic times, as shown in Fig. 8b.
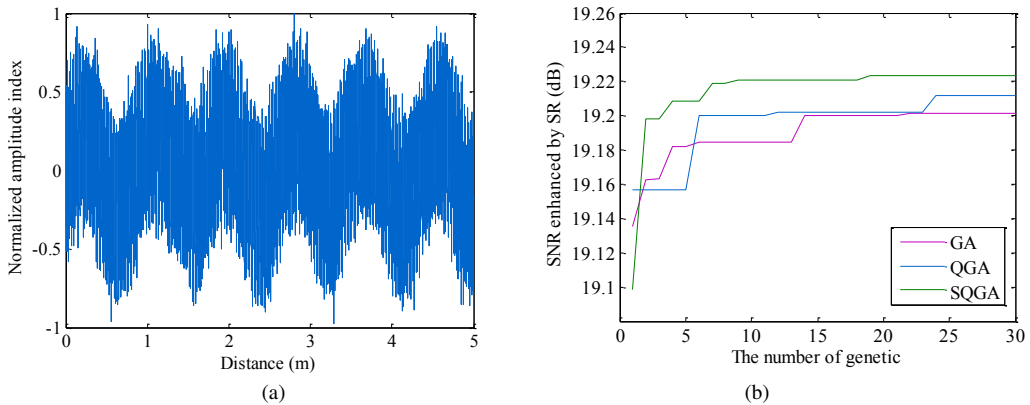

Fig. 8. (a) Time-domain recovery signal. (b) The genetic evolution curves.

Next, we take the three-axis signal of the array center sensor as the research object for OPL processing and we set the reference signal to:

$$R_j(t) = \sin(2\pi f_j t + \pi/6), \qquad (16)$$

where $f_{j=1,2}$ are the lower and higher frequencies of the harmonic excitation signal respectively. In order to ensure the completeness of the algorithm, phase-sensitive detection of the frequency components of the reference signal is carried out with each dimension of the acquisition signal. Then the reference signal is shifted by $\pi/2$ and phase-sensitive detection performed again. The results for the integrator with a cut-off frequency of 15 Hz are shown in Fig. 9(a). It shows that axial and radial signals are more distinct than circumferential. One should note here that actual different defects have different sensitive directions which leads to the target identification being unintuitive. Therefore, we adopted the TF to improve it, as shown in Fig. 9(b).

In addition, the simulation results show that the effectiveness of the algorithm is closely related to SNR. When SNR ≤ 5 dB, the target signal are seriously aliased and the algorithm fails. When SNR ≥ 20 dB, the target signal can be accurately identified, as shown in Fig. 10.
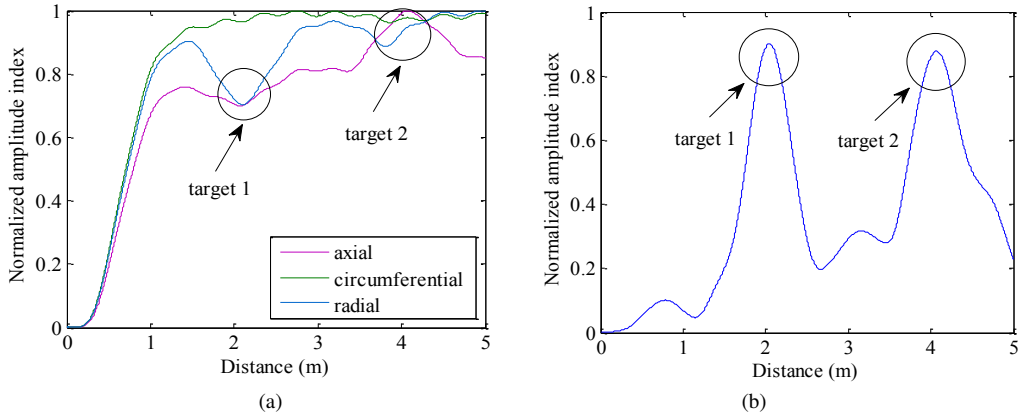
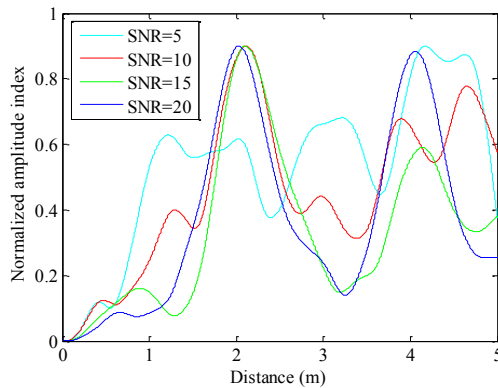Fig. 9. (a) Target signal recognition. (b) Tensor modulus array fusion.

Fig. 10. The effectiveness of OPLTF with different SNR.

5. Experiment and results

5.1. Indoor experiment platform

In order to verify the effectiveness of non-contact harmonic detection of ferromagnetic material defects, an indoor steel pipeline defect detection experimental platform was built. The experimental system consists of an array detector, harmonic excitation source, and a high-speed data acquisition instrument. The experimental platform is shown in Fig. 11.

Q235 seamless steel pipeline was selected as the experimental object, with a total length of 265 cm, an external diameter of 7.5 cm and a wall thickness of 0.5 cm. There were six prefabricated defects on the pipeline wall which were an axial crack, a circumferential crack, a rectangular groove, a circular through hole, a circular blind hole and a 45-degree crack in turn, corresponding to the actual distances of 53 cm, 75 cm, 105 cm, 144 cm, 185 cm and 217 cm respectively. A 5-element TMR 3D vector focused array detector was designed, whose output was in the form of a differential signal and the parallel sampling frequency was 6 000 Hz. During the detection, the lifting height from the detector to the pipeline was 28 cm, and the detector moved forward at a constant speed of 0.5 m/s.
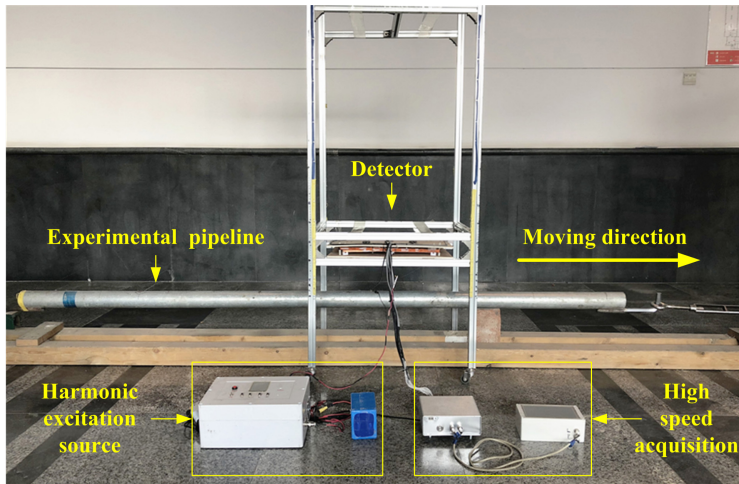
Fig. 11. Experimental platform.

Under the conditions of this experimental platform, two comparative experiments were carried out. In one experiment, the harmonic excitation source was kept on, the lower frequency was 23 Hz, the higher frequency was 1 kHz, and the excitation current was 2.5 A. In the other experiment, the harmonic excitation source was kept off which was the traditional passive detection method without excitation, similar to the GM detection [31].

5.2. Signal analysis and discussion

In order to make analytic effort more efficient, experimental data of 126 cm in the middle part of the pipeline were selected for analysis, including three prefabricated defects, namely, the circumferential crack, the rectangular groove and the circular through hole. These actual defects on the pipeline are shown in Fig. 12.

Fig. 12. The actual pipeline defects types.

In the first experiment, the data collected by the the vector array detector consisted of 15 columns. The three-axis data of the center sensor were taken as reference and the rest of the data were fused. After repeated experiments, we obtained the optimal original signal of the array center sensor by detecting the pipeline which is shown in Fig. 13(a). After taking the radial signal as the research object we show its spectrum in Fig. 13(b) which provides the basis for the selection of a subsequent reference signal frequency. At the same time, it can be seen from the figure that there is no obvious new frequency in the detection data except the natural frequency of the excitation signal.
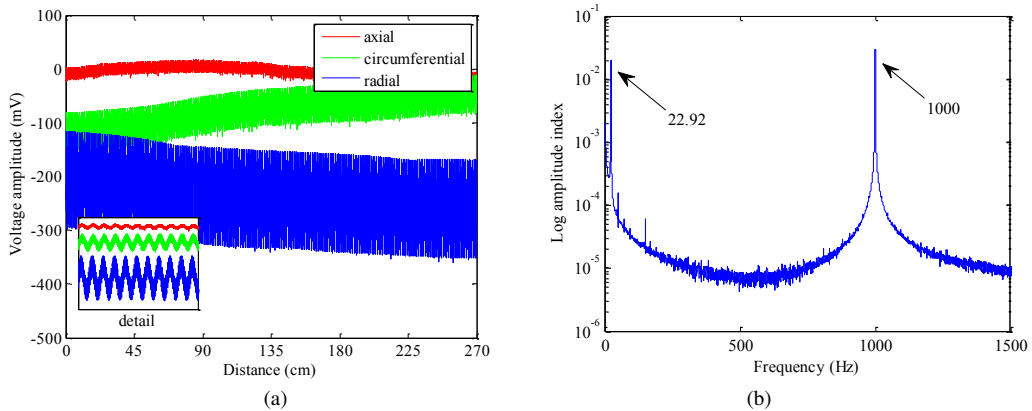
Fig. 13. Experiment 1: (a) original signal; (b) spectrum.

First, the detection data were filtered with a fourth-order Butterworth low-pass of 4 kHz and a normalization recalculation to eliminate the difference of inherent bias between sensors. Then SQGSR was used to improve the SNR of the collected data and enhance the target signal. Finally, OPLTF was used to identify the target signal effectively. In order to highlight the ability of non-contact harmonic detection of ferromagnetic material defect signals, the EEMDSR algorithm was used to compare with the proposed algorithm. The EEMDSR algorithm is composed of EEMD and SR. In this algorithm, EEMD can reduce the influence of modal aliasing, and eliminate the background excitation signal to a certain extent through decomposition and reconstruction. But it causes a loss in target signal energy, and the efficiency of artificial parameter selection in traditional SR is low and the error is large, so this algorithm cannot achieve the effective extraction of harmonic detection damage target signal. The maximum value was used as the basis for defect target identification. There are three peaks in the signal analysis results successively corresponding to 1#, 2# and 3# pipeline defects, as shown in Fig. 14.
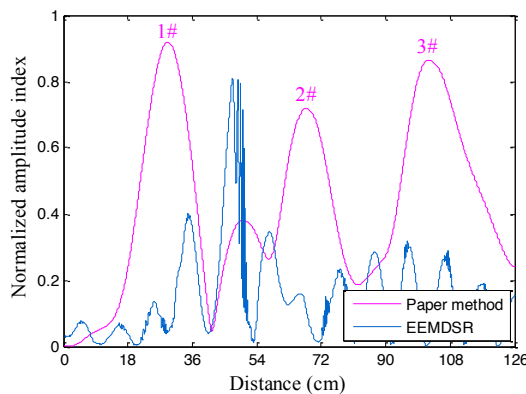

Fig. 14. The signal analysis results of experiment 1.

In the second experiment, the signal with the *best* quality was selected for processing after repeated collection. The original triaxial data of the sensor at the center of the array detector is shown in Fig. 15(a) and its spectrum is shown in Fig. 15(b).
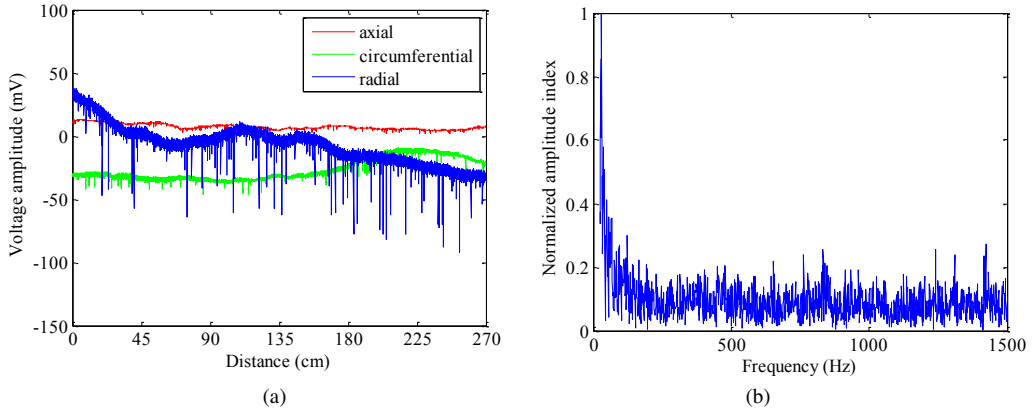
Fig. 15. Experiment 2: (a) original signal; (b) spectrum.

It can be seen from Fig. 15 that the original signal is distorted by noise, especially for the radial signal. Obviously, harmonic detection can play a better role in noise suppression. The energy distribution in the frequency domain is uniform, but the high energy is mainly concentrated in the low frequency band. Therefore, low-pass filtering was performed on the signal with a cut-off frequency of 300 Hz. Then EMD was used to decompose and reconstruct the signal and calculate the gradient. Finally, the sum of squares of the triaxial data was calculated, as shown in Fig. 16.
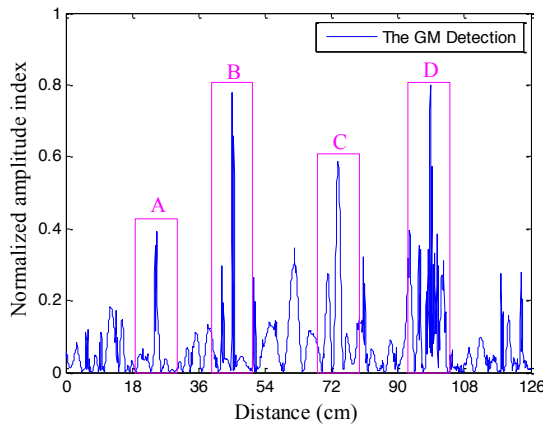

Fig. 16. The signal analysis results of experiment 2.

A, B, C and D are the suspected defect locations. Compared with the actual location of defects on the pipeline, it can be determined that A is not the defect location but an interference signal. In practical engineering applications under unknown conditions, the real defect location discrimination will be directly affected. In addition, after the decomposition and reconstruction of the signal, the target position will be offset, resulting in a large error. The comparison results of the two detection experiments are shown in Table 3. It shows that the proposed method has higher detection precision and stronger defect identification capability than other methods.

Table 3. Error analysis of detection experiment.

Defect type	Circumferential crack	Rectangular groove	Circular through hole
Paper method (cm) / Error (%)	31 / 3.3	65 / 8.3	104 / 4.6
GM detection (cm) / Error (%)	45 / 50.0	73 / 21.7	98 / 10.1
Actual position / cm	30	60	109

6. Conclusions

In this paper, a non-contact harmonic detection method for defects of ferromagnetic materials based on SQGSR and OPLTF is proposed. According to the characteristics of ferromagnetic materials, a high sensitivity vector array focusing detector of TMR was designed which can improve the performance by 2 times. At the same time, the lower frequency of several tens of Hz and higher frequency of several kHz electromagnetic wave characteristics were integrated in the excitation signal which effectively increased the lift-off height and broke through the skin effect limitation. A signal processing algorithm for defect target extraction of ferromagnetic materials is proposed and improved which makes the SNR increase 9.6 times on average with faster convergence speed and higher accuracy. Taking a Q235 steel pipeline as the object of experiment, the detection and identification of three defects were achieved under non-contact conditions with an error of less than 10%. The proposed method provides a novel non-contact electromagnetic NDT idea for identifying defects of ferromagnetic materials and a reference for the detection of subsurface and internal defects.

Acknowledgements

References

[1] Ruibin, G., Wen, J. D., Fei, Q., Min, Y., Zhang, W. G. (2015). Welding residual stress measurement of an urban buried gas pipeline by X-ray diffraction method. *Insight: Non-Destructive Testing & Condition Monitoring*, 57(10), 556–561. https://doi.org/10.1784/insi.2015.57.10.556

[2] Chang, M. K., Sun, H. S., & Ciou, J. C. (2011). Applying Ultrasonic Testing to Detect Hole Defect Near the Surface. *Advanced Materials Research*, *194-196*, 2054–2057. https://doi.org/10.4028/www.scientific.net/amr.194-196.2054

[3] Song, S. P., & Que, P. W. (2006). An effective defect identification scheme in pipeline ultrasonic testing. *Russian Journal of Nondestructive Testing*, *42*(4), 255–260. https://doi.org/10.1134/s1061830906040061

[4] Dai, X., Mo, J. Q., Yin, B., Hu, W., & Wang, S. G. (2013). An automatic magnetic particle inspection system for detecting defects in mooring chains. *Insight: Non-Destructive Testing and Condition Monitoring*, *55*(1), 29–34. https://doi.org/10.1784/insi.2012.55.1.29

[5] Cicic, D. T., Amza, C. G., Popescu, D., & Anania, F. D. (2013). Automated Stand for Non-Destructive Testing Evaluation of Metal Products. *Applied Mechanics and Materials*, *371*, 401–405. https://doi.org/10.4028/www.scientific.net/amm.371.401

[6] Rosado, L. S., Janeiro, F. M., Ramos, P. M., & Piedade, M. (2013). Defect Characterization With Eddy Current Testing Using Nonlinear-Regression Feature Extraction and Artificial Neural Networks. *IEEE Transactions on Instrumentation & Measurement*, *62*(5), 1207–1214. https://doi.org/10.1109/tim.2012.2236729

[7] Ali, K. B., Abdalla, A. N., Rifai, D., & Faraj, M. A. (2017). Review on system development in eddy current testing and technique for defect classification and characterization. *IET Circuits Devices & Systems*, *11*(4), 330–343. https://doi.org/10.1049/iet-cds.2016.0327

[8] Feng, Q. S., Li, R., Nie, B. H., Liu, S. C., Zhao, L. Y., & Zhang, H. (2016). Literature Review: Theory and Application of In-Line Inspection Technologies for Oil and Gas Pipeline Girth Weld Defection. *Sensors*, *17*(1). https://doi.org/10.3390/s17010050

[9] Liu, B., He, L. Y., Zhang, H., Cao, Y., & Fernandes, H. (2017). The axial crack testing model for long distance oil-gas pipeline based on magnetic flux leakage internal inspection method. *Measurement*, *103*, 275–282. https://doi.org/10.1016/j.measurement.2017.02.051

[10] Hu, B., Yu, R., & Liu, J. (2016). Experimental study on the corrosion testing of a buried metal pipeline by transient electromagnetic method. *Anti-Corros Methods Mater.*, *63*(4), 262–268. https://doi.org/10.1108/a cmm-10-2014-1444

[11] Liao, K. X., Quan, K. Y., & Chun, Z.. (2011). Principle and technical characteristics of non-contact magnetic tomography method inspection for oil and gas pipeline. *ICPTT, Sustainable Solutions for Water, Sewer, Gas, And Oil Pipelines*, 1039–1048. https://doi.org/10.1061/41202(423)111

[12] Zhang, T., Wang, X. H., Chen, Y. C., Zia, U., Ju, H. Y., & Zhao, Y. Z. (2019). Non-contact geomagnetic detection using improved complete ensemble empirical mode decomposition with adaptive noise and Teager energy operator. *Electronics*, *8*(3), 309. https://doi.org/10.3390/electronics8030309

[13] Song, Q., Ding, W. X., Peng, H., Gu, J. J., & Shuai, J. (2017). Pipe Defect Detection with Remote Magnetic Inspection and Wavelet Analysis. *Wireless Personal Communications*, *95*(3), 2299–2313. https://doi.org/10.1007/s11277-017-4092-8

[14] Huang, Y. M., Wu, D., Zhang, Z. F., Chen, H. B., & Chen, S. B. (2017). EMD Based Pulsed TIG Welding Process Porosity Defect Detection and Defect Diagnosis using GA-SVM. *Journal of Materials Processing Technology*, *239*, 92–102. https://doi.org/10.1016/j.jmatprotec.2016.07.015

[15] Amirat, Y., Benbouzid, M. E. H., Wang, T., Bacha, K., & Feld, G. (2018). EEMD-based notch filter for induction machine bearing faults detection. *Applied Acoustics*, *133*, 202–209. https://doi.org/10.1016/j.apacoust.2017.12.030

[16] Shi, P. M., Yuan, D. Z., Han, D. Y., Zhang, Y., & Fu, R. R. (2018). Stochastic resonance in a time-delayed feedback tristable system and its application in fault diagnosis. *Journal of Sound Vibration*, *424*, 1–14. https://doi.org/10.1016/j.jsv.2018.03.007

[17] Ryu, C, Kong, S. G., & Kim, H. (2011). Enhancement of feature extraction for low-quality fingerprint images using stochastic resonance. *Pattern Recognition Letters*, *32*(2), 107–113. https://doi.org/10.1016/j.patrec.2010.09.008

[18] He, L. F., Cao, L., Zhang, G., & Yi, T. (2018). Weak signal detection based on underdamped stochastic resonance with an exponential bistable potential. *Chinese Journal of Physics*, *56*, 1588–1598. https://doi.org/10.1016/j.cjph.2018.05.001

[19] Wan, C. B., Pan, M. C., Zhang, Q., Wu, F. H., Pan, L., & Sun, X. Y. (2018). Magnetic Anomaly Detection Based on Stochastic Resonance. *Sensors and Actuators A: Physical*, *278*, 11–17. https://doi.org/10.1016/j.sna.2018.05.009

[20] Shi, P. M., An, S. J., Li, P., & Han, D. Y. (2016). Signal feature extraction based on cascaded multi-stable stochastic resonance denoising and EMD method. *Measurement*, *90*, 318–328. https://doi.org/10.1016/j.measurement.2016.04.073

[21] Hong, K. L., Chang, B. H., Reza, M., & Xiong, Z. L. (2018). Weak Defect Identification for Centrifugal Compressor Blade Crack Based on Pressure Sensors and Genetic Algorithm. *Sensors*, *18*(4), 1264. https://doi.org/10.3390/s18041264

[22] Yin, G., Zhang, Y. T., Fan, H. B., Ren, G. Q., & Li, Z. N. (2015). One-step calibration of magnetic gradient tensor system with nonlinear least square method. *Sensors & Actuators A Physical*, *229*, 77–85. https://doi.org/10.1016/j.sna.2015.03.026

[23] Yin, G., Zhang, Y. T., Fan, H. B., Ren, G. Q., & Li, Z. N. (2015). Integrated calibration of magnetic gradient tensor system. *Journal of Magnetism and Magnetic Materials*, *374*, 289–297. https://doi.org/10.1016/j.jmmm.2014.08.022

[24] Fartookzadeh, M. (2019). Serial-fed linear frequency diverse arrays for obtaining direction of arrival (DOA) of frequency modulated continuous waveform (FMCW) sources with ambiguity reduction. *International Journal of RF and Microwave Computer-Aided Engineering*, *29*(10), e21900. https://doi.org/10.1002/mmce.21900

[25] Wang, S., Wang, F. Z., Wang, S., & Li, G. J. (2018). Detection of multi-frequency weak signals with adaptive stochastic resonance system. *Chinese Journal of Physics*, *56*(3): 994–1000. https://doi.org/10.1016/j.cjph.2018.04.001

[26] Lai, Z. H., & Leng, Y. G. (2016). Weak-signal detection based on the stochastic resonance of bistable duffing oscillator and its application in incipient fault diagnosis. *Mechanical Systems & Signal Processing*, *81*, 60–74. https://doi.org/10.1016/j.ymssp.2016.04.002

[27] Zhu, X. T., Xiong, J. B., & Liang, Q. (2018). Fault Diagnosis of Rotation Machinery based on Support Vector Machine Optimized by Quantum Genetic Algorithm. *IEEE Access*, *6*. https://doi.org/10.1109/access.2018.2789933

[28] Jin, Z. F., Hou, Z. Q., Yu, W. S., & Wang, X. (2018). Target tracking approach via quantum genetic algorithm. *IET Computer Vision*, *12*(3), 241–251. https://doi.org/10.1049/iet-cvi.2017.0176

[29] Monica, T., Rajasekhar, A., Pant, M., & Abraham, A. (2011). Enhancing the Local Exploration Capabilities of Artificial Bee Colony Using Low Discrepancy Sobol Sequence. *Communications in Computer & Information Science*, *168*, 158–168. https://doi.org/10.1007/978-3-642-22606-9_19

[30] Sui, Y. Y., Leslie, K., & Clark, D. (2017). Multiple-Order Magnetic Gradient Tensors for Localization of a Magnetic Dipole. *IEEE Magnetics Letters*, *8*, 1–5. https://doi.org/10.1109/lmag.2017.2708682

[31] Dubov, A. A., Dubov, AI. A., & Kolokolnikov, S. M. (2017). Non-contact magnetometric diagnostics of potentially hazardous sections of buried and insulated pipelines susceptible to failure. *Welding in the World*, *61*(1), 107–115. https://doi.org/10.1007/s40194-016-0402-0
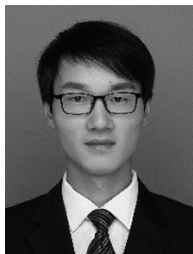
Yizhen Zhao is a Ph.D. student at the Beijing University of Technology, Faculty of Materials and Manufacturing-College of Mechanical Engineering and Applied Electronics Technology.
His main research interests include modern measurement and control technology, signal processing algorithms and intelligent diagnosis systems.
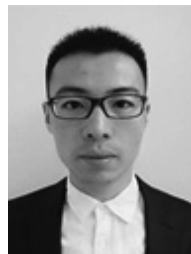
Haiyang Ju is a Ph.D. student at the Beijing University of Technology, Faculty of Materials and Manufacturing-College of Mechanical Engineering and Applied Electronics Technology.
His main research interests include signal processing algorithms and pipeline non-destructive testing.

Xinhua Wang is a Ph.D., professor and doctoral supervisor at the Beijing University of Technology, Faculty of Materials and Manufacturing-College of Mechanical Engineering and Applied Electronics Technology.
His main research interests include pipeline inspection technology and safety evaluation, pipeline corrosion and protection, fluid transmission and control technology.

Shuai Yi is a postdoctor at the Beijing University of Technology, Faculty of Materials and Manufacturing-College of Mechanical Engineering and Applied Electronics Technology.
His main research interests include pipeline inspection technology and integrity assessment.

Yingchun Chen is a Ph.D., associate professor and master supervisor at the Beijing University of Technology, Faculty of Materials and Manufacturing-College of Mechanical Engineering and Applied Electronics Technology.
His main research interests include oil and gas pipeline stray current corrosion detection, pipeline damage detection and pipe mechanics.